

Gravitational form factors of the deuteron

J. Yu. Panteleeva,¹ E. Epelbaum,¹ A. M. Gasparyan,¹ and J. Gegelia^{1,2}

¹*Institut für Theoretische Physik II, Ruhr-Universität Bochum, D-44780 Bochum, Germany*

²*Tbilisi State University, 0186 Tbilisi, Georgia*

(Dated: 25 November, 2024)

The gravitational form factors of the deuteron are calculated in the framework of non-relativistic chiral effective field theory. Non-relativistic reduction of the matrix element of the energy-momentum tensor operator for spin-one systems is worked out, and the gravitational form factors of the deuteron are extracted from the three-point function of the energy-momentum tensor using the LSZ reduction formula. The obtained form factors are compared to results of model calculations available in the literature.

This paper is dedicated to memory of our dear teacher, friend and colleague Maxim Polyakov. It provides new insights into the structure of hadronic and nuclear systems encoded in the gravitational form factors, the activity that has been initiated by Maxim.

I. INTRODUCTION

It's a great honor to contribute to this special issue of Acta Physica Polonica B dedicated to the memory of Mitya Diakonov, Vitya Petrov and Maxim Polyakov. These virtuosos of theoretical physics left deep and lasting footprints in the field of QCD, and they also played a central role in shaping the research directions of our institute. One of us (E.E.) came across Mitya, Vitya and Maxim in the middle of 1990s, when he came to Bochum as a student. While working on different topics, it was a truly unforgettable experience to enjoy a unique, scientifically-vivid atmosphere of the TPII-institute with lively discussions in the “Strong interaction room” and intense Russian-style seminars. For a personal recollection of this time see also a recent paper by another former TPII member Hyun-Chul Kim [1].

In the last decade, the main scientific connection between Maxim's and our groups at the TPII-institute was, of course, the chiral physics. Over the years, Maxim was also continuously interested (among a plethora of other things) in probing internal structure of hadrons with gravity-induced interactions, see [2, 3] for some of his seminal contributions to the field. Naturally, he came to the idea to approach this problem using the language of the effective chiral Lagrangian, generalized to curved space-time [4]. This was how our way-too-short collaboration with Maxim on this topic started [5–7].

This paper represents a next logical step towards uncovering the structure of strongly interacting systems with gravitational probes. Specifically, we focus here on the gravitational form factors (GFFs) of the simplest nuclear system, the deuteron, using the framework of chiral effective field theory (EFT). Triggered by the seminal papers by Weinberg [8, 9], it offers a systematic formalism with a controlled improvable accuracy. For recent reviews see, e.g., Refs. [10–13]. While the electromagnetic structure of the deuteron has already been extensively analyzed in the EFT framework using various approaches [14–22], the GFFs have, to the best of our knowledge, been only considered in model calculations using a phenomenological nucleon-nucleon potential [23, 24], see also Ref. [25] for a related discussion. In the present work we fill this gap and extract the GFFs of the deuteron by calculating the three-point function of the energy-momentum tensor (EMT) in chiral EFT and applying the Lehmann-Symanzik-Zimmermann (LSZ) reduction formalism in analogy to Refs. [14, 20]. We employ the non-relativistic formulation of chiral EFT with pions and nucleons as the only dynamical degrees of freedom.

Our calculation is restricted to the leading-order (LO) nucleon-nucleon (NN) potential which, according to Weinberg's power counting, is given by derivative-less contact interactions and the one-pion-exchange. Non-relativistic expressions for the EMT insertions at LO, next-to-leading order (NLO) and next-to-next-to-leading order (NNLO) are obtained from the corresponding Lorentz-invariant expressions by applying the standard heavy baryon reduction.

Our paper is organized as follows. In section II we briefly outline a general formalism to calculate the deuteron form factors in quantum field theory. The integral equations for the deuteron structure functions are discussed in section III, while the actual calculation of the GFFs is presented in section IV. A brief summary of the most important results of this study is provided in section V.

II. GRAVITATIONAL FORM FACTORS OF THE DEUTERON

Matrix elements of conserved EMT operator for spin-1 systems can be parameterized in terms of six GFFs – the coefficient functions $A_{0,1}(q^2)$, $D_{0,1}(q^2)$, $J(q^2)$ and $E(q^2)$ of the independent conserved Lorentz structures [26]:

$$\begin{aligned}
t_{\mu\nu} &= \langle p', \sigma' | \hat{T}_{\mu\nu}(0) | p, \sigma \rangle = 2P_\mu P_\nu \left[-\epsilon' \cdot \epsilon A_0(q^2) + \frac{P \cdot \epsilon' P \cdot \epsilon}{M^2} A_1(q^2) \right] \\
&+ 2 \left[P_\mu (\epsilon'_\nu P \cdot \epsilon + \epsilon_\nu P \cdot \epsilon') + P_\nu (\epsilon'_\mu P \cdot \epsilon + \epsilon_\mu P \cdot \epsilon') \right] J(q^2) + \frac{1}{2} (q_\mu q_\nu - g_{\mu\nu} q^2) \left[\epsilon' \cdot \epsilon D_0(q^2) + \frac{P \cdot \epsilon' P \cdot \epsilon}{M^2} D_1(q^2) \right] \\
&+ \left[\frac{1}{2} q^2 (\epsilon_\mu \epsilon'_\nu + \epsilon'_\mu \epsilon_\nu) - (\epsilon'_\nu q_\mu + \epsilon'_\mu q_\nu) \epsilon \cdot P + (\epsilon_\nu q_\mu + \epsilon_\mu q_\nu) \epsilon' \cdot P - 4g_{\mu\nu} P \cdot \epsilon' P \cdot \epsilon \right] E(q^2), \tag{1}
\end{aligned}$$

where (p, σ) and (p', σ') are the (four-momentum, spin index) quantum numbers of the initial and final states, respectively, $q = p' - p$ is the momentum transfer, $P = (p + p')/2$, while $\epsilon'^\beta \equiv \epsilon^{*\beta}(p', \sigma')$ and $\epsilon^\beta \equiv \epsilon^\beta(p, \sigma)$ are the polarization vectors. Further, M is a mass scale introduced to render the GFFs dimensionless. It is often taken equal to the mass of the system m . However, to avoid mixing of orders in the non-relativistic $1/m$ -expansion, we prefer to distinguish between two mass parameters until the non-relativistic reduction is performed. The one-particle states $|p, \sigma\rangle$ satisfy the normalization condition

$$\langle p', \sigma' | p, \sigma \rangle = 2p^0 (2\pi)^3 \delta^3(\mathbf{p} - \mathbf{p}') \delta_{\sigma\sigma'}. \tag{2}$$

Up-to-and-including zeroth order in the $1/m$ expansion (corresponding to static approximation) for the kinematics with $P^i = 0$, we obtain the following expressions [27]:

$$\begin{aligned}
t^{00} &= 2m^2 \left[\delta_{\sigma'\sigma} \left(\mathcal{E}_0(-\mathbf{q}^2) + \frac{\mathbf{q}^2}{3M^2} \mathcal{E}_2(-\mathbf{q}^2) \right) - \frac{q_{\sigma'} q_\sigma}{M^2} \mathcal{E}_2(-\mathbf{q}^2) \right], \\
t^{0i} &= -m \mathcal{J}(-\mathbf{q}^2) (\delta_{i\sigma'} q_\sigma - \delta_{i\sigma} q_{\sigma'}), \\
t^{ij} &= 2 \left[\mathcal{D}_2(-\mathbf{q}^2) \left(\delta_{ij} q_\sigma q_{\sigma'} - \frac{1}{2} q^i (q_\sigma \delta_{j\sigma'} + q_{\sigma'} \delta_{j\sigma}) - \frac{1}{2} q^j (q_\sigma \delta_{i\sigma'} + q_{\sigma'} \delta_{i\sigma}) + \frac{\mathbf{q}^2}{2} (\delta_{i\sigma} \delta_{j\sigma'} + \delta_{i\sigma'} \delta_{j\sigma}) \right) \right. \\
&\quad \left. + (\mathbf{q}^2 \delta_{ij} - q_i q_j) \left\{ \delta_{\sigma'\sigma} \left(\mathcal{D}_0(-\mathbf{q}^2) - \frac{2}{3} \mathcal{D}_2(-\mathbf{q}^2) + \frac{\mathbf{q}^2}{3M^2} \mathcal{D}_3(-\mathbf{q}^2) \right) - \frac{q_{\sigma'} q_\sigma}{M^2} \mathcal{D}_3(-\mathbf{q}^2) \right\} \right], \tag{3}
\end{aligned}$$

where the combinations of the form factors are given by

$$\begin{aligned}
\mathcal{E}_0(-\mathbf{q}^2) &= A_0(-\mathbf{q}^2) - \frac{\mathbf{q}^2}{12M^2} A_1(-\mathbf{q}^2), \\
\mathcal{E}_2(-\mathbf{q}^2) &= \frac{A_1(-\mathbf{q}^2)}{4}, \\
\mathcal{J}(-\mathbf{q}^2) &= J(-\mathbf{q}^2), \\
\mathcal{D}_0(-\mathbf{q}^2) &= \frac{D_0(-\mathbf{q}^2)}{4} + \frac{\mathbf{q}^2}{48M^2} D_1(-\mathbf{q}^2) - \frac{E(-\mathbf{q}^2)}{3}, \\
\mathcal{D}_2(-\mathbf{q}^2) &= -\frac{E(-\mathbf{q}^2)}{2}, \\
\mathcal{D}_3(-\mathbf{q}^2) &= -\frac{D_1(-\mathbf{q}^2)}{16}. \tag{4}
\end{aligned}$$

Above, we have chosen the Cartesian basis for three-dimensional polarization vectors.

Using Eq. (3), we extract below the GFFs of the deuteron from the three-point function of the EMT operator $\hat{T}^{\mu\nu}$ and two interpolating fields of the deuteron,

$$G_{\sigma'\sigma}^{\mu\nu}(p', p) = \int d^4x d^4y e^{-ip' \cdot y} e^{ip \cdot x} \langle 0 | T \left[\mathcal{D}_\sigma^\dagger(x) \hat{T}^{\mu\nu}(0) \mathcal{D}_{\sigma'}(y) \right] | 0 \rangle, \tag{5}$$

using the LSZ reduction formula [14]

$$\langle p', \sigma' | \hat{T}^{\mu\nu} | p, \sigma \rangle = -\frac{1}{Z} \left[(p^2 - M_d^2) (p'^2 - M_d^2) G_{\sigma'\sigma}^{\mu\nu}(p', p) \right]_{p^2, p'^2 \rightarrow M_d^2}, \tag{6}$$

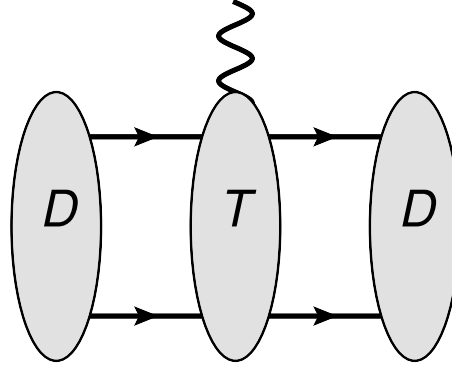


FIG. 1: Three-point function of the EMT operator and two interpolating fields of the deuteron. Ellipses with D represent the amplitudes of the deuteron interpolating field interacting with a pair of nucleon fields, while T stands for the two-nucleon-irreducible part of the vertex function. Solid and wavy lines denote the nucleons and the EMT insertion, respectively.

where $M_d = 2m_N - E_b$ is the deuteron mass, E_b is its binding energy, m_N refers to the nucleon mass, while Z is the residue of the deuteron propagator. The deuteron interpolating field in Eq. (5) is defined as [14]

$$\mathcal{D}_i \equiv N^T \mathcal{P}_i N = \sum_{\alpha, \beta, a, b=1}^2 N_{\alpha, a} \mathcal{P}_{i, ab}^{\alpha\beta} N_{\beta, b}, \quad \mathcal{P}_i \equiv \frac{1}{\sqrt{8}} \sigma_2 \sigma_i \tau_2, \quad (7)$$

where α, β and a, b are the spin and isospin indices, respectively. Notice that observable quantities do not depend on a particular form of interpolating fields. The two-point function of the deuteron interpolating fields is given by

$$G_{\mathcal{D}}(p) \delta_{\sigma'\sigma} = \int d^4x e^{-ipx} \langle 0 | T [\mathcal{D}_{\sigma'}^\dagger(x) \mathcal{D}_\sigma(0)] | 0 \rangle = \delta_{\sigma'\sigma} \frac{i 2M_d Z}{p^2 - M_d^2 + i\epsilon} + \text{N.P.}, \quad (8)$$

where "N. P." stands for contributions without the deuteron pole. The vertex function $G_{\sigma'\sigma}^{\mu\nu}(p', p)$ can be represented diagrammatically as shown in Fig. 1.

III. THE DEUTERON EQUATION

Below we briefly summarize the derivation of the equation for the deuteron structure functions of Ref. [20], applied to the non-relativistic case. In non-relativistic low-energy EFT, the NN scattering amplitude is obtained by solving the integral equation

$$T(\mathbf{p}', \mathbf{p}) = V(\mathbf{p}', \mathbf{p}) - m_N \int \frac{d^3\mathbf{k}}{(2\pi)^3} \frac{V(\mathbf{p}', \mathbf{k}) T(\mathbf{k}, \mathbf{p})}{m_N E - \mathbf{k}^2 + i\epsilon}, \quad (9)$$

where $E = \mathbf{p}^2/m_N$ denotes the energy of two incoming nucleons in the center-of-mass frame.

For our calculations, we need the amplitude of the deuteron interpolating field interacting with a pair of nucleon fields. This quantity in the rest frame of the deuteron is given by

$$D_j(\mathbf{p}') = \mathcal{P}_j + m_N \int \frac{d^3\mathbf{k}}{(2\pi)^3} \frac{\mathcal{P}_j T(\mathbf{p}', \mathbf{k})}{m_N E - \mathbf{k}^2 + i\epsilon}, \quad (10)$$

where the NN scattering amplitude $T(\mathbf{p}', \mathbf{p})$ is obtained by solving Eq. (9). The amplitude $D(\mathbf{p}')$ can be parameterized in terms of two structure functions Δ_1 and Δ_2 via

$$D_j(\mathbf{p}') = \Delta_1(\mathbf{p}'^2) \mathcal{P}_j + p'_a p'_b \Delta_2(\mathbf{p}'^2) (\sigma^a)^T \mathcal{P}_j \sigma^b, \quad (11)$$

where we do not show the isospin indices and terms resulting from anti-symmetrization. Notice that the structure functions Δ_1 and Δ_2 can be easily related to the S - and D -state components of the deuteron wave function (see also Ref. [28]). To obtain equations for the structure functions $\Delta_{1,2}$ we parameterize the NN potential by indicating explicitly the spin indices:

$$V_{\alpha\beta, \gamma\delta}(\mathbf{p}', \mathbf{p}) = v^0(\mathbf{p}', \mathbf{p}) \delta_{\alpha\gamma} \delta_{\beta\delta} + v_a^1(\mathbf{p}', \mathbf{p}) (\sigma_{\alpha\gamma}^a \delta_{\beta\delta} + \delta_{\alpha\gamma} \sigma_{\beta\delta}^a) + v_{ab}^2(\mathbf{p}', \mathbf{p}) \sigma_{\alpha\gamma}^a \sigma_{\beta\delta}^b, \quad (12)$$

where

$$\begin{aligned}
v^0(\mathbf{p}', \mathbf{p}) &= \nu_1(\mathbf{p}', \mathbf{p}), \\
v_a^1(\mathbf{p}', \mathbf{p}) &= i \epsilon^{abc} p^b p'^c \nu_3(\mathbf{p}', \mathbf{p}), \\
v_{ab}^2(\mathbf{p}', \mathbf{p}) &= \delta_{ab} \nu_2(\mathbf{p}', \mathbf{p}) + p'^a p'^b \nu_5(\mathbf{p}', \mathbf{p}) + p^a p^b \nu_6(\mathbf{p}', \mathbf{p}) + (p^a p'^b + p'^a p^b) \nu_4(\mathbf{p}', \mathbf{p}),
\end{aligned} \tag{13}$$

and $\nu_i(\mathbf{p}', \mathbf{p})$ are scalar functions of \mathbf{p}'^2 , \mathbf{p}^2 and $\mathbf{p}' \cdot \mathbf{p}$. For the structure functions, we obtain the following system of integral equations:

$$\begin{aligned}
\Delta_1(\mathbf{p}^2) &= 1 + m_N \int \frac{d^3 \mathbf{k}}{(2\pi)^3} G(\mathbf{k}) \left\{ \Delta_1(\mathbf{k}^2) [\nu_1(\mathbf{p}, \mathbf{k}) + \nu_2(\mathbf{p}, \mathbf{k}) + C_1 \nu_6(\mathbf{p}, \mathbf{k})] \right. \\
&\quad + \Delta_2(\mathbf{k}^2) \left[C_1 (\nu_1(\mathbf{p}, \mathbf{k}) + \nu_2(\mathbf{p}, \mathbf{k})) + 2(\mathbf{p} \cdot \mathbf{k}) \nu_3(\mathbf{p}, \mathbf{k}) + 2\mathbf{k}^2 (\mathbf{p} \cdot \mathbf{k}) \nu_4(\mathbf{p}, \mathbf{k}) \right. \\
&\quad \left. \left. + [(\mathbf{p} \cdot \mathbf{k})^2 - C_1 \mathbf{p}^2] \nu_5(\mathbf{p}, \mathbf{k}) + (\mathbf{k}^2)^2 \nu_6(\mathbf{p}, \mathbf{k}) \right] \right\}, \\
\Delta_2(\mathbf{p}^2) &= m_N \int \frac{d^3 \mathbf{k}}{(2\pi)^3} G(\mathbf{k}) \left\{ \Delta_1(\mathbf{k}^2) [2B \nu_4(\mathbf{p}, \mathbf{k}) + C_2 \nu_6(\mathbf{p}, \mathbf{k}) + \nu_5(\mathbf{p}, \mathbf{k})] \right. \\
&\quad \left. + \Delta_2(\mathbf{k}^2) \left[C_1 \nu_5(\mathbf{p}, \mathbf{k}) - 2B \mathbf{k}^2 \nu_3(\mathbf{p}, \mathbf{k}) + C_2 (\nu_1(\mathbf{p}, \mathbf{k}) + \nu_2(\mathbf{p}, \mathbf{k}) + 2(\mathbf{p} \cdot \mathbf{k}) \nu_3(\mathbf{p}, \mathbf{k})) \right] \right\},
\end{aligned} \tag{14}$$

where

$$B \equiv \frac{\mathbf{p} \cdot \mathbf{k}}{\mathbf{p}^2}, \quad C_1 \equiv \frac{1}{2} \left[\mathbf{k}^2 - \frac{(\mathbf{p} \cdot \mathbf{k})^2}{\mathbf{p}^2} \right], \quad C_2 \equiv \frac{3(\mathbf{p} \cdot \mathbf{k})^2 - \mathbf{k}^2 \mathbf{p}^2}{2\mathbf{p}^4}. \tag{15}$$

For our calculations of the deuteron GFFs we consider the regulated leading-order NN potential of chiral EFT given by

$$V_0(\mathbf{p}', \mathbf{p}) = (C_S + C_T \boldsymbol{\sigma}_1 \cdot \boldsymbol{\sigma}_2) \frac{\Lambda^4}{(\mathbf{p}'^2 + \Lambda^2)(\mathbf{p}^2 + \Lambda^2)} - \frac{g_A^2}{4F_\pi^2} \boldsymbol{\tau}_1 \cdot \boldsymbol{\tau}_2 \frac{\boldsymbol{\sigma}_1 \cdot (\mathbf{p}' - \mathbf{p}) \boldsymbol{\sigma}_2 \cdot (\mathbf{p}' - \mathbf{p})}{(\mathbf{p}' - \mathbf{p})^2 + M_\pi^2} \frac{\Lambda^2 - M_\pi^2}{(\mathbf{p}' - \mathbf{p})^2 + \Lambda^2}, \tag{16}$$

which corresponds to

$$\begin{aligned}
\nu_1(\mathbf{p}', \mathbf{p}) &= C_S \frac{\Lambda^4}{(\mathbf{p}'^2 + \Lambda^2)(\mathbf{p}^2 + \Lambda^2)}, \\
\nu_2(\mathbf{p}', \mathbf{p}) &= C_T \frac{\Lambda^4}{(\mathbf{p}'^2 + \Lambda^2)(\mathbf{p}^2 + \Lambda^2)}, \\
\nu_3(\mathbf{p}', \mathbf{p}) &= 0, \\
\nu_4(\mathbf{p}', \mathbf{p}) &= \frac{g_A^2}{4F_\pi^2} \boldsymbol{\tau}_1 \cdot \boldsymbol{\tau}_2 \frac{1}{(\mathbf{p}' - \mathbf{p})^2 + M_\pi^2} \frac{\Lambda^2 - M_\pi^2}{(\mathbf{p}' - \mathbf{p})^2 + \Lambda^2}, \\
\nu_5(\mathbf{p}', \mathbf{p}) &= -\frac{g_A^2}{4F_\pi^2} \boldsymbol{\tau}_1 \cdot \boldsymbol{\tau}_2 \frac{1}{(\mathbf{p}' - \mathbf{p})^2 + M_\pi^2} \frac{\Lambda^2 - M_\pi^2}{(\mathbf{p}' - \mathbf{p})^2 + \Lambda^2}, \\
\nu_6(\mathbf{p}', \mathbf{p}) &= -\frac{g_A^2}{4F_\pi^2} \boldsymbol{\tau}_1 \cdot \boldsymbol{\tau}_2 \frac{1}{(\mathbf{p}' - \mathbf{p})^2 + M_\pi^2} \frac{\Lambda^2 - M_\pi^2}{(\mathbf{p}' - \mathbf{p})^2 + \Lambda^2},
\end{aligned} \tag{17}$$

where C_S and C_T are low-energy coupling constants of the leading-order NN contact interaction Lagrangian [8, 9], g_A is the nucleon axial charge, while M_π and F_π are the mass and the decay constant of the pion, respectively. In the above expressions, we have introduced a smooth cutoff with a parameter Λ to regularize ultraviolet divergences. The employed regulator for the one-pion-exchange potential does not modify its longest-range part (i.e., the left-hand cut in the on-shell partial-wave two-nucleon amplitude closest to the physical region) and the physics related to it [29, 30]. For the same reason, we adopted the effective value of the axial coupling constant $g_A = 1.29$ [31] that takes into account the Goldberger-Treiman discrepancy. Note that our regularization procedure violates EMT conservation, which could potentially lead to the appearance of contributions to the form factors proportional to positive powers of Λ , which cannot be absorbed by counter terms of the effective Lagrangian allowed by symmetries. However, as we will see from our results, such effects appear to be rather small. A more systematic approach can

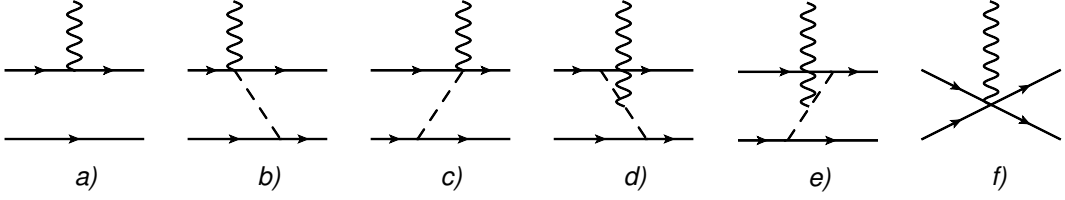


FIG. 2: Tree-level diagrams contributing to the vertex function of the EMT operator. Diagrams where the graviton couples to the second nucleon line are not shown. Solid, dashed and wavy lines correspond to nucleons, pions and gravitons, respectively.

be developed by applying a symmetry-preserving regularization [32–34], which however goes beyond the scope of the current work. We set the numerical value of the cutoff parameter of the order of the EFT expansion breakdown scale $\Lambda \sim \Lambda_b \sim 400 - 600$ MeV [35–38]. To analyze the sensitivity of our results to the choice of the cutoff, we vary it within this range $\Lambda \in (400, 600)$ MeV. For the central cutoff value, we choose $\Lambda = 500$ MeV.

To calculate the residue of the two-point function of the deuteron interpolating fields it is useful to write the dressed deuteron propagator $G_{\mathcal{D}}$ using Eq. (11) as

$$G_{\mathcal{D}}(E, \mathbf{0}) = m_N \int \frac{d^3 \mathbf{k}}{(2\pi)^3} \frac{\tilde{\Delta}_1(\mathbf{k}^2)}{m_N E - \mathbf{k}^2 + i\epsilon} + \text{N. P.}, \quad (18)$$

where $\tilde{\Delta}_1(\mathbf{k}^2) = \Delta_1(\mathbf{k}^2) + \frac{\mathbf{k}^2}{3} \Delta_2(\mathbf{k}^2)$ and "N. P." stands for the non-pole part.

IV. CALCULATION OF THE FORM FACTORS

In this section we calculate the matrix element of the EMT in the Breit frame for the initial and final deuteron states with the quantum numbers $(-\mathbf{q}/2, \sigma)$ and $(\mathbf{q}/2, \sigma')$. For the matrix element, we obtain

$$\langle \mathbf{q}/2, \sigma' | \hat{T}_{\mu\nu} | -\mathbf{q}/2, \sigma \rangle = m_N^2 \int \frac{d^3 k_1}{(2\pi)^3} \frac{d^3 k_2}{(2\pi)^3} \frac{D_{\sigma', cd}^{\gamma\delta}(\mathbf{k}_2) T_{\mu\nu}^{cd, \gamma\delta; ab, \alpha\beta}(\frac{\mathbf{q}}{4} + \mathbf{k}_2, \frac{\mathbf{q}}{4} - \mathbf{k}_2; \mathbf{k}_1 - \frac{\mathbf{q}}{4}, -\mathbf{k}_1 - \frac{\mathbf{q}}{4}) D_{\sigma, ab}^{\dagger, \alpha\beta}(\mathbf{k}_1)}{(\mathbf{k}_1^2 + p_B^2)(\mathbf{k}_2^2 + p_B^2)}, \quad (19)$$

where $p_B = \sqrt{m_N E_b}$ is the deuteron binding momentum and the arguments of the amplitude in the integrand correspond to the individual momenta of both nucleons. Comparing the results of calculating the expression of Eq. (19) with the parameterization of Eq. (3) we extract the GFFs of the deuteron in the static approximation.

To calculate the order-by-order approximations to the deuteron matrix element of the EMT we apply the standard Weinberg power counting for the few-body sector of chiral EFT [8, 9] to the integral in Eq. (19), see, e.g., Refs. [39, 40] for details. According to this power counting, the pion mass and external three-momenta (divided by Λ_b) count as of order one, each internal pion (nucleon) line counts as of order minus two (minus one), the nucleon mass counts as of order minus one (NN power counting, see Refs. [8–10, 13] for details) and a noninteracting spectator nucleon counts as of order minus three. Each pionic loop adds four to the overall chiral order. Interaction vertices originating from the effective Lagrangian of order N count as of chiral order N , while the vertices corresponding to EMT have different orders for different components. The EMT corresponding to the first-order Lorentz-invariant Lagrangian generates the vertices with contributions starting with the order minus one, all other N -th order Lagrangians lead to N -th or higher order contributions in the corresponding EMT vertices, modulo (enhanced) factors of the nucleon mass in terms with derivatives acting on nucleon field. The relevant single-nucleon effective Lagrangian and the corresponding expression for the energy-momentum tensor can be found in Ref. [4].

In our calculation, we include all diagrams shown in Fig. 2, which contain contributions to the vertex function up to zeroth order in all components of the $T_{\mu\nu}$ part in the integrand of Eq. (19). Note that chiral expansion for different components of the deuteron matrix element of EMT starts at different orders. In particular, the expansion for the 00-th component starts at order -4 , whereas the leading contributions to the $0i$ -th and ij -th components come from orders -2 and 0 , respectively.

In a fully consistent approach, one would have to include also higher-order corrections to the nucleon-nucleon potential (T -matrix) as well as relativistic corrections to the nucleon propagator, at least for T_{00} and T_{0i} . Obviously, in the present exploratory study, such an unnecessary complication would provide us with no additional information. Therefore, we stick to the leading-order NN potential and drop the relativistic corrections to the nucleon propagator for all gravitational form factors.

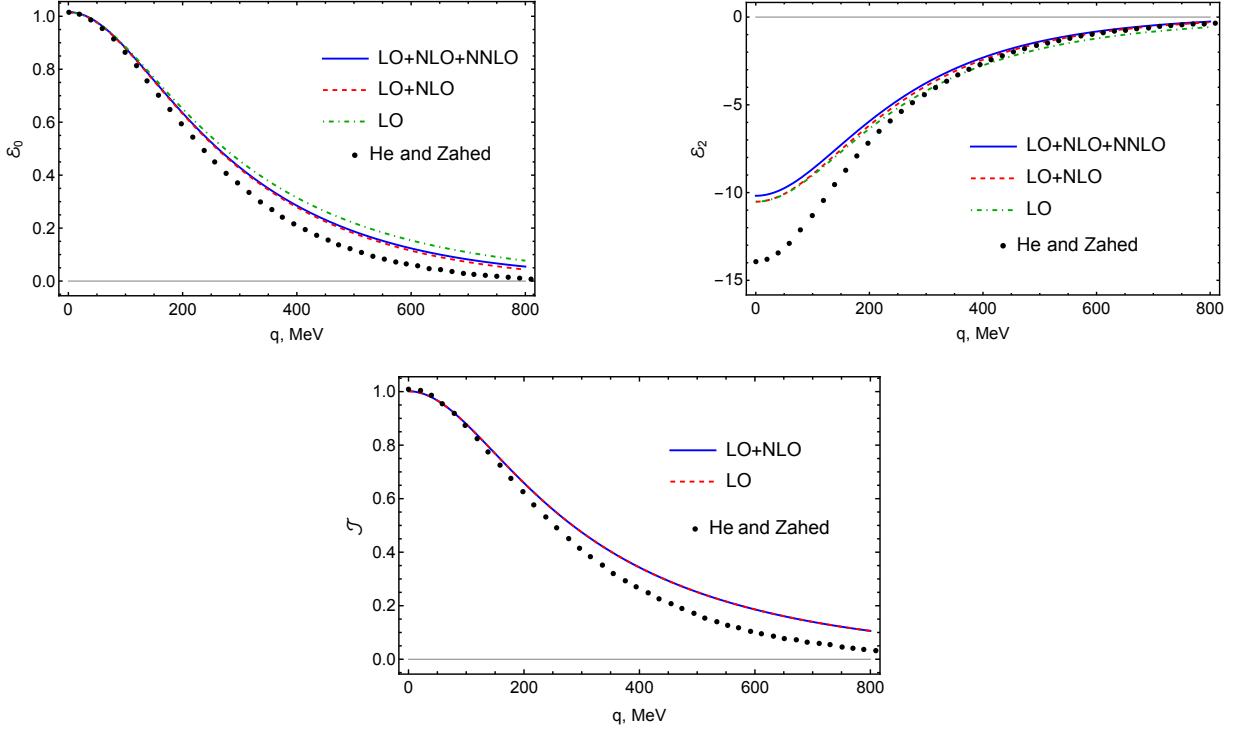


FIG. 3: Numerical results for the gravitational form factors \mathcal{E} and \mathcal{J} of the deuteron using the cutoff parameter $\Lambda = 500$ MeV. Definitions of the EFT orders are given in text. We compare our results with the GFFs by He and Zahed given in Fig. 3 of Ref. [23]. Notice that our two curves for \mathcal{J} coincide due to vanishing NLO contribution to this form factor.

The leading contribution to the form factors is given by diagram a) in Fig. 2 (and its partner diagram where the graviton couples to another nucleon) with one EMT insertion in a single nucleon line. It has the following form:

$$\langle \mathbf{q}/2, \sigma' | \hat{T}_{\mu\nu}^{\text{LO}} | -\mathbf{q}/2, \sigma \rangle = 4m_N^2 \int \frac{d^3k}{(2\pi)^3} \frac{D_{\sigma'}(\mathbf{k} + \mathbf{q}/4) T_{\mu\nu,a}(\mathbf{k} + \mathbf{q}/2, \mathbf{k} - \mathbf{q}/2) D_{\sigma}^{\dagger}(\mathbf{k} - \mathbf{q}/4)}{[(\mathbf{k} + \mathbf{q}/4)^2 + p_B^2][(\mathbf{k} - \mathbf{q}/4)^2 + p_B^2]}, \quad (20)$$

where, up to the accuracy of our calculation, we have:

$$\begin{aligned} T_{00,a}(\mathbf{k} + \mathbf{q}/2, \mathbf{k} - \mathbf{q}/2) &= m_N + \frac{\mathbf{k}^2}{2m_N} - \frac{i\epsilon^{lmn}\sigma^l k^m q^n}{4m_N} + c_8 \frac{\mathbf{q}^2}{4} + 2c_9 \mathbf{q}^2, \\ T_{0i,a}(\mathbf{k} + \mathbf{q}/2, \mathbf{k} - \mathbf{q}/2) &= k_i + \frac{i\epsilon_{ilm}\sigma^l q^m}{4} + \frac{c_9}{m_N} [\mathbf{q}^2 k_i + (\mathbf{k} \cdot \mathbf{q}) q_i], \\ T_{ij,a}(\mathbf{k} + \mathbf{q}/2, \mathbf{k} - \mathbf{q}/2) &= \frac{k_i k_j}{m_N} + \frac{i\sigma^l q^m}{4m_N} (k_i \epsilon_{jlm} + k_j \epsilon_{ilm}) - \frac{c_8}{4} [\mathbf{q}^2 \delta_{ij} - q_i q_j]. \end{aligned} \quad (21)$$

Here, c_8 and c_9 are coupling constants of the subleading pion-nucleon Lagrangian in curved spacetime [4] and $\mathbf{k} - \mathbf{q}/2$ and $\mathbf{k} + \mathbf{q}/2$ denote three-momenta of the incoming and outgoing states of the nucleon, respectively. Currently, there is no way to estimate the value of the low-energy constant c_9 , so we set $c_9 = 0$ in all numerical calculations. In the power counting scheme we employ, the disconnected contributions stemming from the diagram a) of Fig. 2 are of orders -4 , -2 , -1 and 0 .

The connected two-nucleon diagrams in Fig. 2 are all of chiral order zero. The regularized contributions of diagrams b) and c) to the vertex function $T_{\mu\nu}(\mathbf{k}_2 + \mathbf{q}/4, -\mathbf{k}_2 + \mathbf{q}/4; \mathbf{k}_1 - \mathbf{q}/4, -\mathbf{k}_1 - \mathbf{q}/4)$ at the accuracy of our calculations have the following form (graviton coupling to both, the upper and lower vertices):

$$\begin{aligned} T_{00,b+c} &= -\frac{g_A^2 \tau_1 \cdot \tau_2}{F_\pi^2} \frac{\sigma_1 \cdot \tilde{\mathbf{k}} \sigma_2 \cdot \tilde{\mathbf{k}} \Lambda^2 - M_\pi^2}{\tilde{\mathbf{k}}^2 + M_\pi^2} \frac{\Lambda^2 - M_\pi^2}{\tilde{\mathbf{k}}^2 + \Lambda^2}, \\ T_{0i,b+c} &= 0, \\ T_{ij,b+c} &= -\frac{g_A^2 \tau_1 \cdot \tau_2}{4F_\pi^2} \left[\frac{\sigma_1 \cdot \tilde{\mathbf{k}}}{\tilde{\mathbf{k}}^2 + M_\pi^2} (-2\delta_{ij} \sigma_2 \cdot \tilde{\mathbf{k}} + \tilde{k}^i \sigma_2^j + \tilde{k}^j \sigma_2^i) + \frac{\sigma_2 \cdot \tilde{\mathbf{k}}}{\tilde{\mathbf{k}}^2 + M_\pi^2} (-2\delta_{ij} \sigma_1 \cdot \tilde{\mathbf{k}} + \tilde{k}^i \sigma_1^j + \tilde{k}^j \sigma_1^i) \right] \frac{\Lambda^2 - M_\pi^2}{\tilde{\mathbf{k}}^2 + \Lambda^2}, \end{aligned} \quad (22)$$

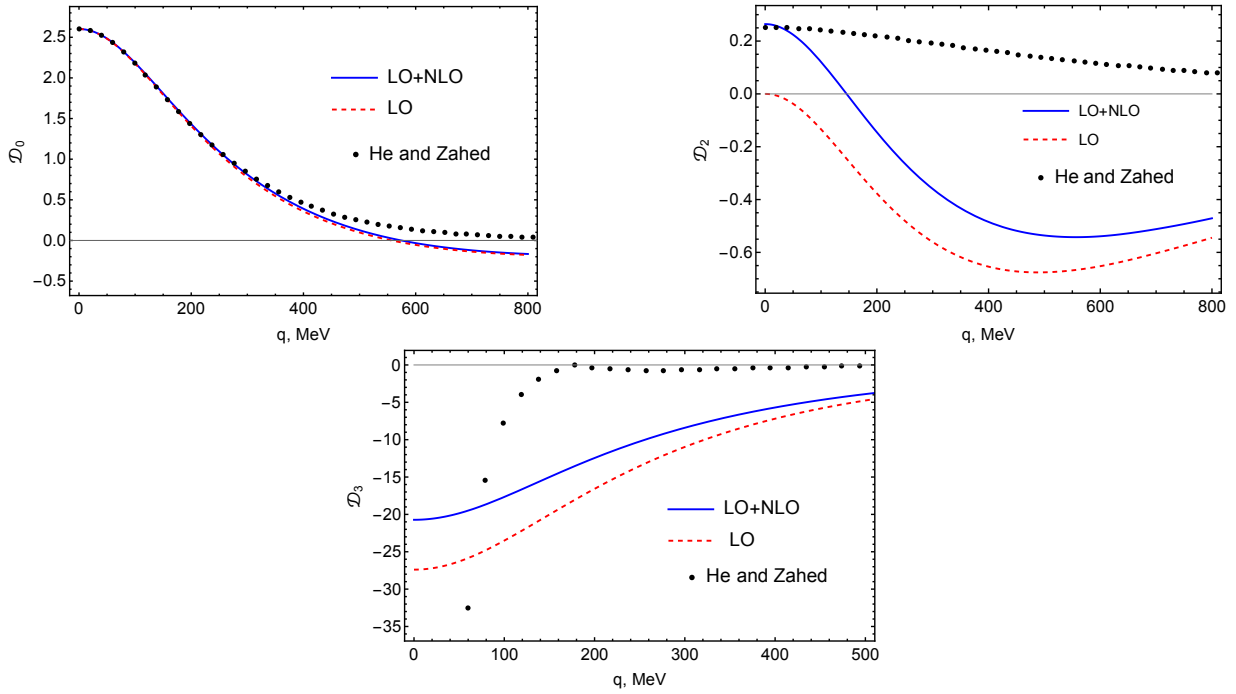


FIG. 4: Numerical results for the gravitational form factors \mathcal{D}_i using the cutoff parameter $\Lambda = 500$ MeV. Definitions of the EFT orders are given in text. We compare our results with the GFFs by He and Zahed given in Fig. 3 of Ref. [23].

The regularized contributions of diagrams d) and e) have the form:

$$\begin{aligned}
 T_{00,d+e} &= \frac{g_A^2 \tau_1 \cdot \tau_2}{4F_\pi^2} \frac{\sigma_1 \cdot \bar{\mathbf{k}} \sigma_2 \cdot \tilde{\mathbf{k}}}{(\bar{\mathbf{k}}^2 + M_\pi^2)(\tilde{\mathbf{k}}^2 + M_\pi^2)} \left[M_\pi^2 + \bar{\mathbf{k}} \cdot \tilde{\mathbf{k}} \right] \frac{\Lambda^2 - M_\pi^2}{\bar{\mathbf{k}}^2 + \Lambda^2} \frac{\Lambda^2 - M_\pi^2}{\tilde{\mathbf{k}}^2 + \Lambda^2}, \\
 T_{0i,d+e} &= 0, \\
 T_{ij,d+e} &= \frac{g_A^2 \tau_1 \cdot \tau_2}{4F_\pi^2} \frac{\sigma_1 \cdot \bar{\mathbf{k}} \sigma_2 \cdot \tilde{\mathbf{k}}}{(\bar{\mathbf{k}}^2 + M_\pi^2)(\tilde{\mathbf{k}}^2 + M_\pi^2)} \left[-\delta_{ij}(M_\pi^2 + \bar{\mathbf{k}} \cdot \tilde{\mathbf{k}}) + \bar{k}^i \tilde{k}^j + \bar{k}^j \tilde{k}^i \right] \frac{\Lambda^2 - M_\pi^2}{\bar{\mathbf{k}}^2 + \Lambda^2} \frac{\Lambda^2 - M_\pi^2}{\tilde{\mathbf{k}}^2 + \Lambda^2}, \quad (23)
 \end{aligned}$$

and the result of diagram f), which corresponds to the coupling of the EMT to the leading order NN contact interaction vertex, reads:

$$T_{\mu\nu,f} = -2(C_S + C_T)g^{\mu\nu}, \quad (24)$$

where we used the shorthand notation with $\bar{\mathbf{k}} = \mathbf{k}_1 - \mathbf{k}_2 - \mathbf{q}/2$ and $\tilde{\mathbf{k}} = \mathbf{k}_1 - \mathbf{k}_2 + \mathbf{q}/2$. Notice that the one-loop corrections to the single-nucleon EMT are also formally of order zero. However, their contributions result merely in the renormalization of the nucleon mass, nucleon field and the c_8 and c_9 coupling constants. We have not shown the one-pion-exchange two-nucleon irreducible diagrams where the EMT couples to a single nucleon line, because their contributions are canceled by $1/m_N$ corrections to the one-pion-exchange nucleon-nucleon potential. This is completely analogous to the well-known cancellation of the analogous time-ordered perturbation theory contribution to the three-nucleon force at NLO by iterations of the one-pion-exchange potential including the $1/m_N$ correction, see, e.g., Ref. [41].

Using the above expressions, we calculated the GFFs of the deuteron by solving the integral equations for the deuteron amplitudes and calculating the matrix elements of EMT numerically. We fixed the coupling constant of the S -wave nucleon-nucleon contact interaction by reproducing the binding energy of the deuteron. In Figs. 3 and 4, we show our results using $\Lambda = 500$ MeV together with the results of Ref. [23] for the deuteron GFFs in the parameterization of Eq. (3).¹ The notation for chiral orders of various form factors follows from the explicit expressions for the matrix elements in Eqs. (21)-(23):

¹ Notice that while we plot the figures for q up to 800 MeV to compare to Ref. [23], our chiral EFT results cannot be trusted at such large values of the momentum transfer.

- For the form factors \mathcal{E}_0 and \mathcal{E}_2 , the LO contribution involves diagram a) apart from the c_8 term that forms the NLO contribution, while the remaining diagrams constitute the NNLO terms.
- For the form factor \mathcal{J} , the whole contribution up to the accuracy of our calculation is generated by diagram a).
- For the form factors \mathcal{D}_0 , \mathcal{D}_2 and \mathcal{D}_3 , the LO term emerges from diagram a) proportional to c_8 , while the remaining nonvanishing diagrams contribute at NLO.

Our calculated form factors \mathcal{E}_0 , \mathcal{E}_2 and \mathcal{J} show, as functions of $q = |\mathbf{q}|$, a similar behavior to those of Ref. [23]. Note that the deviation from 1 of the \mathcal{E}_0 form factor at $q = 0$ (corresponding to the mass of the deuteron) is tiny, which indicates that the effect of the violation of the EMT conservation due to the noninvariant regularization and the neglected relativistic corrections is rather small. We fixed the value of the coupling constant c_8 to $c_8 = -2.77 \text{ GeV}^{-1}$, such that our calculated value of $\mathcal{D}_0(0)$ coincides with that of Ref. [23]. The extracted value of c_8 is of natural size, which allows us to analyze convergence of the chiral expansion. The resulting q -dependence of our form factor \mathcal{D}_0 is very similar to that of Ref. [23]. On the other hand, our curve for \mathcal{D}_2 has a different shape, while the form factor \mathcal{D}_3 shows qualitatively different behavior. This is because the results of Ref. [23], when recalculated in the GFFs of the parameterization of Eq. (3), lead to \mathcal{D}_3 which has a singular behavior at the origin, while this is not the case for our results. We checked that our numerical results show a very mild cutoff dependence for values of Λ between ~ 400 and 600 MeV . The variation of the form factors is comparable with or smaller than the highest-order contribution considered. As argued above, residual cutoff dependence is expected to be further reduced if a symmetry-preserving regulator is used.

The curves in Figs. 3, 4 demonstrate a reasonable convergence rate of the chiral expansion for the deuteron gravitational form factors when going from the LO to NLO and then to NNLO results. The only exception of the rapid convergence is the small- q region of the form factor \mathcal{D}_3 , which is caused by the fact that the leading-order term proportional to the c_8 coupling constant vanishes at $q = 0$. One of the factors that accelerate the convergence is a small typical momentum of the nucleons inside the deuteron (due to its small binding energy), which enters the convolution integrals in Eqs. (19) and (20).

V. SUMMARY

In this work, we have calculated the GFFs of the deuteron in the framework of chiral effective field theory with pions and nucleons as dynamical degrees of freedom. We extracted the GFFs by applying the standard LSZ formalism to the three-point function of the EMT operator and the deuteron interpolating fields. To obtain the deuteron "wave function" in momentum space, we modified the system of integral equations for the deuteron of Ref. [20] by adjusting it to our non-relativistic approach. To regularize the nucleon-nucleon potential consisting of the contact interaction and the one-pion-exchange parts, as well as the two-nucleon diagrams contributing to the EMT, we applied a smooth cutoff regularization.

We solved the integral equations for the deuteron, calculated the matrix element of the EMT numerically, and compared the obtained GFFs of the deuteron to the results of Ref. [23] by recalculating the latter in terms of our parameterization. We have fixed the free parameter c_8 that appears in our calculations by fitting it to the value of $\mathcal{D}_0(0)$ from Ref. [23] and determined the coupling constant of the S -wave nucleon-nucleon contact interaction by reproducing the binding energy of the deuteron. The results of two calculations are found to show a similar behavior as functions of the momentum transfer for \mathcal{E}_0 , \mathcal{E}_2 , \mathcal{D}_0 and \mathcal{J} , while the GFF for \mathcal{D}_2 shows a different pattern. As for the form factor \mathcal{D}_3 , the (recalculated) result of Ref. [23] has a singular behavior for vanishing q while $\mathcal{D}_3(0)$ is finite in our case. We have observed a rather rapid convergence of the chiral expansion for the gravitational form factors of the deuteron and a mild cutoff dependence of the results.

Acknowledgments

We thank the authors of Ref. [23] for providing us with their calculated numerical results for the deuteron GFFs. This work was supported in part by ERC NuclearTheory (grant No. 885150), by BMBF (Grant No. 05P21PCFP1), by the MKW NRW under the funding code NW21-024-A, by DFG and NSFC through funds provided to the Sino-German CRC 110 "Symmetries and the Emergence of Structure in QCD" (NSFC Grant No. 11621131001, DFG Project-ID 196253076 - TRR 110), by the Georgian Shota Rustaveli National Science Foundation (Grant No. FR-23-856) and

by the EU Horizon 2020 research and innovation program (STRONG-2020, grant agreement No. 824093).

-
- [1] H. C. Kim, [arXiv:2411.13292 [hep-ph]].
 - [2] M. V. Polyakov, Phys. Lett. B **555**, 57-62 (2003) [arXiv:hep-ph/0210165 [hep-ph]].
 - [3] M. V. Polyakov and P. Schweitzer, Int. J. Mod. Phys. A **33**, no.26, 1830025 (2018) [arXiv:1805.06596 [hep-ph]].
 - [4] H. Alharazin, D. Djukanovic, J. Gegelia and M. V. Polyakov, Phys. Rev. D **102**, no.7, 076023 (2020) [arXiv:2006.05890 [hep-ph]].
 - [5] J. Gegelia and M. V. Polyakov, Phys. Lett. B **820**, 136572 (2021) [arXiv:2104.13954 [hep-ph]].
 - [6] E. Epelbaum, J. Gegelia, U.-G. Meißner and M. V. Polyakov, Phys. Rev. D **105**, no.1, 016018 (2022) [arXiv:2109.10826 [hep-ph]].
 - [7] E. Epelbaum, J. Gegelia, N. Lange, U.-G. Meißner and M. V. Polyakov, Phys. Rev. Lett. **129**, no.1, 012001 (2022) [arXiv:2201.02565 [hep-ph]].
 - [8] S. Weinberg, Phys. Lett. B **251**, 288 (1990).
 - [9] S. Weinberg, Nucl. Phys. **B363**, 3 (1991).
 - [10] E. Epelbaum, H.-W. Hammer and U.-G. Meißner, Rev. Mod. Phys. **81**, 1773 (2009), [arXiv:0811.1338 [nucl-th]].
 - [11] R. Machleidt and D. R. Entem, Phys. Rept. **503**, 1 (2011), [arXiv:1105.2919 [nucl-th]].
 - [12] H.-W. Hammer, S. König and U. van Kolck, Rev. Mod. Phys. **92**, no.2, 025004 (2020), [arXiv:1906.12122 [nucl-th]].
 - [13] E. Epelbaum, H. Krebs and P. Reinert, Front. in Phys. **8**, 98 (2020), [arXiv:1911.11875 [nucl-th]].
 - [14] D. B. Kaplan, M. J. Savage and M. B. Wise, Phys. Rev. C **59**, 617 (1999), [nucl-th/9804032].
 - [15] D. R. Phillips and T. D. Cohen, Nucl. Phys. A **668**, 45 (2000), [nucl-th/9906091].
 - [16] M. Walz and U.-G. Meißner, Phys. Lett. B **513**, 37 (2001), [nucl-th/0103020].
 - [17] D. R. Phillips, Phys. Lett. B **567**, 12 (2003), [nucl-th/0304046].
 - [18] D. R. Phillips, J. Phys. G **34**, 365 (2007), [nucl-th/0608036].
 - [19] S. Kölling, E. Epelbaum and D. R. Phillips, Phys. Rev. C **86**, 047001 (2012), [arXiv:1209.0837 [nucl-th]].
 - [20] E. Epelbaum, A. M. Gasparyan, J. Gegelia and M. R. Schindler, Eur. Phys. J. A **50**, 51 (2014), [arXiv:1311.7164 [nucl-th]].
 - [21] A. A. Filin, V. Baru, E. Epelbaum, H. Krebs, D. Möller and P. Reinert, Phys. Rev. Lett. **124**, no.8, 082501 (2020), [arXiv:1911.04877 [nucl-th]].
 - [22] A. A. Filin, D. Möller, V. Baru, E. Epelbaum, H. Krebs and P. Reinert, Phys. Rev. C **103**, no.2, 024313 (2021), [arXiv:2009.08911 [nucl-th]].
 - [23] F. He and I. Zahed, Phys. Rev. C **110**, no.1, 014312 (2024), [arXiv:2401.09318 [nucl-th]].
 - [24] F. He and I. Zahed, Phys. Rev. C **109**, no.4, 045209 (2024), [arXiv:2310.12315 [nucl-th]].
 - [25] A. Freese and W. Cosyn, Phys. Rev. D **106** (2022) no.11, 114013 [arXiv:2207.10787 [hep-ph]].
 - [26] M. V. Polyakov and B. D. Sun, Phys. Rev. D **100** (2019) no.3, 036003, [arXiv:1903.02738 [hep-ph]].
 - [27] J. Y. Panteleeva, E. Epelbaum, J. Gegelia and U.-G. Meißner, JHEP **07**, 237 (2023), [arXiv:2305.01491 [hep-ph]].
 - [28] I. Fachruddin, C. Elster and W. Glöckle, Phys. Rev. C **63**, 054003 (2001), [nucl-th/0101009].
 - [29] P. Reinert, H. Krebs and E. Epelbaum, Eur. Phys. J. A **54**, no.5, 86 (2018), [arXiv:1711.08821 [nucl-th]].
 - [30] A. M. Gasparyan, M. F. M. Lutz and E. Epelbaum, Eur. Phys. J. A **49**, 115 (2013), [arXiv:1212.3057 [nucl-th]].
 - [31] E. Epelbaum, W. Glöckle and U.-G. Meißner, Nucl. Phys. A **747**, 362-424 (2005), [arXiv:nucl-th/0405048 [nucl-th]].
 - [32] D. Djukanovic, M. R. Schindler, J. Gegelia and S. Scherer, Phys. Rev. D **72**, 045002 (2005), [arXiv:hep-ph/0407170 [hep-ph]].
 - [33] D. Djukanovic, J. Gegelia, S. Scherer and M. R. Schindler, Few Body Syst. **41**, 141-155 (2007), [arXiv:nucl-th/0609055 [nucl-th]].
 - [34] H. Krebs and E. Epelbaum, Phys. Rev. C **110**, no.4, 044004 (2024), [arXiv:2312.13932 [nucl-th]].
 - [35] E. Epelbaum, H. Krebs and U.-G. Meißner, Eur. Phys. J. A **51**, no.5, 53 (2015), [arXiv:1412.0142 [nucl-th]].
 - [36] R. J. Furnstahl, N. Klco, D. R. Phillips and S. Wesolowski, Phys. Rev. C **92**, no.2, 024005 (2015), [arXiv:1506.01343 [nucl-th]].
 - [37] E. Epelbaum, J. Golak, K. Hebeler, H. Kamada, H. Krebs, U.-G. Meißner, A. Nogga, P. Reinert, R. Skibiński and K. Topolnicki, *et al.* Eur. Phys. J. A **56**, no.3, 92 (2020), [arXiv:1907.03608 [nucl-th]].
 - [38] E. Epelbaum, PoS **CD2018**, 006 (2019) doi:10.22323/1.317.0006
 - [39] E. Epelbaum, Eur. Phys. J. A **34**, 197-214 (2007), [arXiv:0710.4250 [nucl-th]].
 - [40] H. Krebs, Eur. Phys. J. A **56**, no.9, 234 (2020), [arXiv:2008.00974 [nucl-th]].
 - [41] U. van Kolck, Phys. Rev. C **49**, 2932-2941 (1994).